

Supporting Information

Stochastic Differential Scanning Calorimetry by Nonlinear Optical Microscopy

Alex M. Sherman[†], Andreas C. Geiger[†], Casey J. Smith[†], Lynne S. Taylor[‡], Jeremy Hinds[§], Paul A. Stroud[§], and Garth J. Simpson^{*,†}

[†]Department of Chemistry, Purdue University, 560 Oval Drive, West Lafayette, Indiana 47907, United States

[‡]Department of Industrial and Physical Pharmacy, Purdue University, 575 Stadium Mall Drive, West Lafayette, Indiana 47907, United States

[§]Eli Lilly & Company, 1200 W. Morris Street, Indianapolis, IN 46221, United States

*Email address: gsimpson@purdue.edu

TABLE OF CONTENTS

Figure S1. Full SDSC Measurement of Urea

Figure S2. SDSC Video of Urea (AVI)

Figure S3. Distribution of Urea Crystal Volumes

Equations S1-S3. Description of the least-squares fit to recover the IRF of the DSC instrument

Figure S4. Summed Images of Trehalose Dihydrate

Figure S5. SDSC Video of Trehalose Dihydrate (AVI)

Figure S6. IRF Analysis of Trehalose Dihydrate

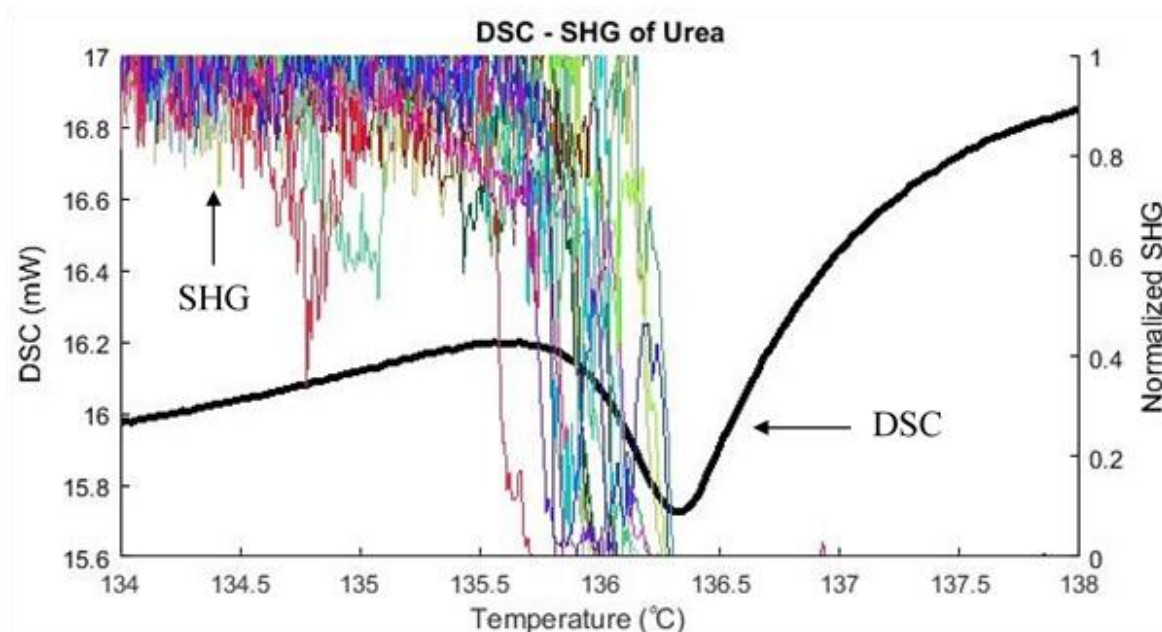


Figure S1. Full SDSC Measurement of Urea. SDSC analysis of urea by combined SHG microscopy and DSC. The solid black line is the DSC trace of the melting of urea with endothermic direction being down (left-axis). The thin colored lines show the normalized SHG intensity of individual urea particles (right-axis), acquired concurrently with DSC measurements. DSC and SHG measurements both indicate a structural transformation in the same temperature range.

Figure S2. SDSC Video of Urea (AVI)

The images collected for urea from SHG microscopy, the per-particle image analysis of the SHG data, and the thermal analysis data by DSC were correlated in time and combined together into a single SDSC video. DSC measurements and the SHG measurements were plotted from 134 °C to 138 °C to capture the melting point of urea with a ramp rate of 10 °C/min. SHG images collected at a rate of 17 frames per second were displayed concurrently to the other data. Video speeds were adjusted to highlight the regions of interest slowing down at the onset of melting and returning to normal speed once the sample had completely melted.

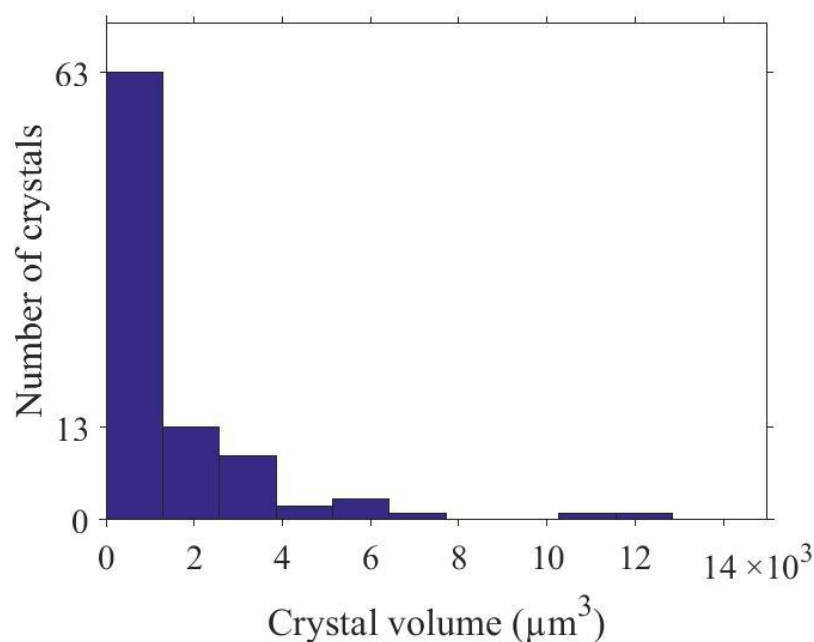


Figure S3. Distribution of Urea Crystal Volumes. The nucleation rate is calculated based on the number of phase transformations observed in the field of view (FoV) per unit time and the estimated mass of the crystals in the FoV. The estimated mass of the crystals comes from the known density of urea and the estimated volume of the crystals, which is calculated from the crystal cross-sectional area (assuming rod-like shape). The distribution of crystal volumes in the FoV are shown in **Figure S3**. A total mass of $0.39 \mu\text{g}$ was calculated from the sum of these volumes multiplied by the density of urea (1.32 g/cm^3). The mass combined with the observed nucleation rate of 6.13 nuclei/s yields the nucleation rate of $1.6 \pm 0.2 \times 10^4 \text{ nuclei per second per milligram}$. The uncertainty in the nucleation rate arises from the number of crystals counted in the FoV, which is dictated by Poisson statistics. The standard deviation, σ of a Poisson distribution with a mean, μ is equal to $\sqrt{\mu}$. We assume the mean of the distribution is approximately equal to the number of crystals counted (58), yielding a standard deviation of ~ 7.6 . When propagated into nucleation rate, it results in an uncertainty of $\pm 0.2 \times 10^4 \text{ nuclei per second per milligram}$.

Equations S1-S3. Description of the least-squares fit to recover the IRF of the DSC instrument

The DSC response was modeled as a convolution between the impulse response function (IRF) of the DSC instrument and the impulsive single-crystal melting events, as measured by SHG microscopy. The DSC model is shown in **Equation S1**.

$$f_{DSC} = x \otimes f_{IRF} \quad (S1)$$

where x is a set of impulses corresponding to the single-crystal melting events measured by SHG microscopy. We assumed a double-exponential IRF, shown in **Equation S2**, consistent with heat flow through a thermal resistor.

$$f_{IRF} = \begin{cases} e^{-\frac{(t-t_0)}{\tau_1}}, & t < t_0 \\ e^{-\frac{(t-t_0)}{\tau_2}}, & t \geq t_0 \end{cases} \quad (S2)$$

where t is time, τ_1 and τ_2 are the characteristic time constants of the two exponentials, and t_0 is the offset time. To recover parameters τ_1 , τ_2 , and t_0 , a least-squares fit was performed to minimize **Equation S3**.

$$\hat{a} = \arg \min_a \left\| y - x \otimes f_{IRF}(a) \right\|^2 \quad (S3)$$

where a is the set of parameters to be minimized (τ_1 , τ_2 , and t_0), \hat{a} is the set of minimized parameters, and y is the experimental DSC trace. Minimization of **Equation S3** resulted in the plot labeled “Convolution” in **Figure 3** (in the manuscript) and recovered parameters of 1.161 ± 0.019 s, 0.435 ± 0.013 s, and 3.088 ± 0.013 s were computed for τ_1 , τ_2 , and t_0 respectively.

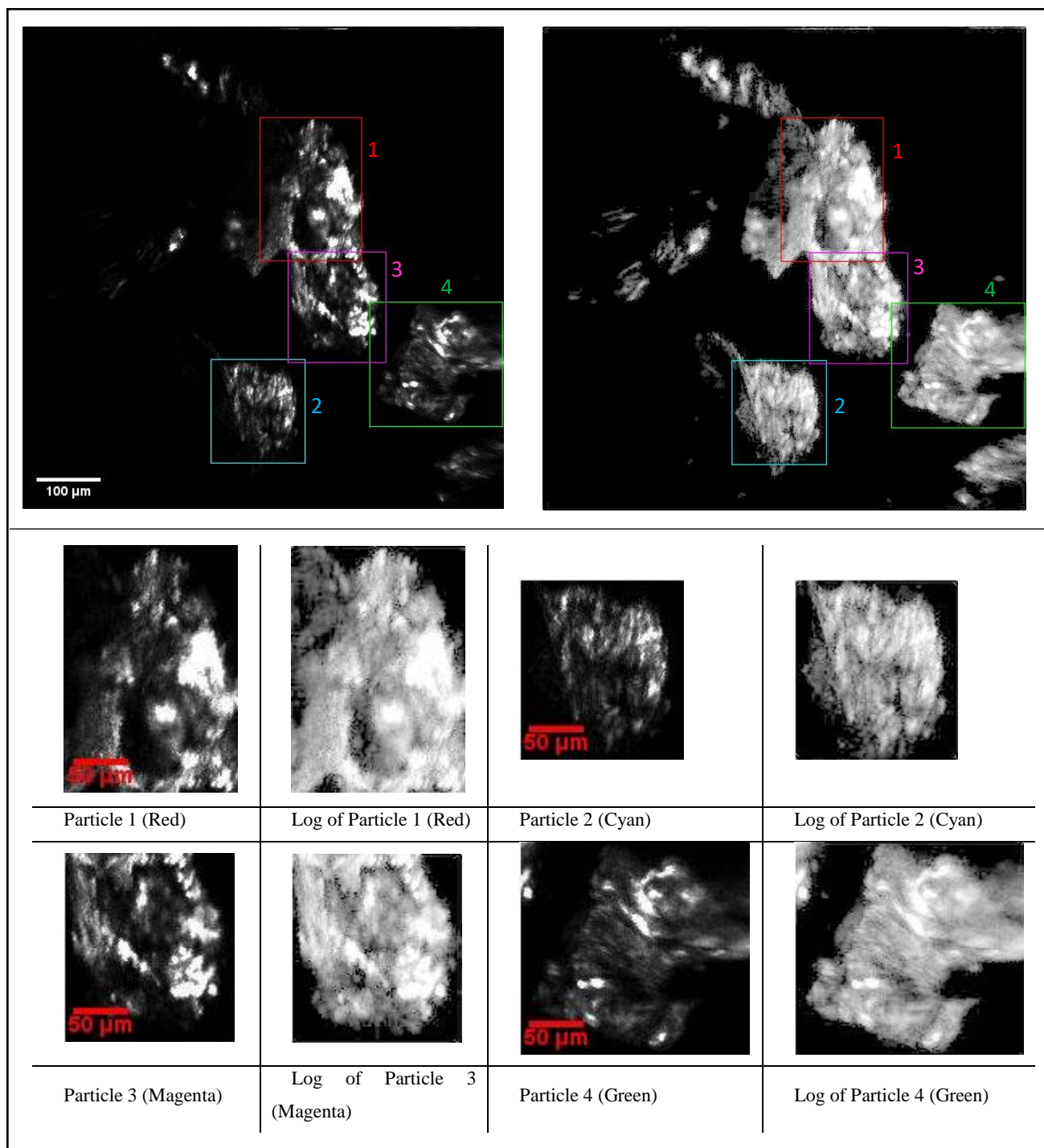


Figure S4. Summed Images of Trehalose Dihydrate. **a)** For the SDSC measurements of trehalose dihydrate, the SHG images collected in the temperature range of 140 °C to 220 °C were summed together to better display the analyzed particles. This temperature range was chosen since each of the particles had high SHG activity for the majority of this region for an extended number of images. Once the images had been summed, the logarithm of this summed image was also displayed to better differentiate between trehalose and background. Boxes were overlaid in the summed images corresponding to the regions of each of the measured particles in the image analysis. **b)** The total FOV was cropped to display the regions corresponding to the four measured particles. For each of these cropped regions, both the summed image and logarithm of this image are displayed.

Figure S5. SDSC Video of Trehalose Dihydrate (AVI)

The images collected for trehalose dihydrate from SHG microscopy, the per-particle image analysis of the SHG data, and the thermal analysis data by DSC were correlated in time and combined together into a single SDSC video. DSC measurements and the SHG measurements were plotted from 80 °C to 240 °C with a ramp rate of 20 °C/min. Colored boxes were overlaid on the SHG images that corresponding to the measured regions of each particle with the colors corresponding to its SHG intensity trace. At approximately 170 °C, a particle briefly moves in and out of the FOV and was ignored in the image analysis. SHG images collected at a rate of 17 frames per second were displayed concurrently with the other data. Video speeds were adjusted to highlight the regions of greatest interest slowing down at the onset of melting and returning to normal speed once the sample completely melted.

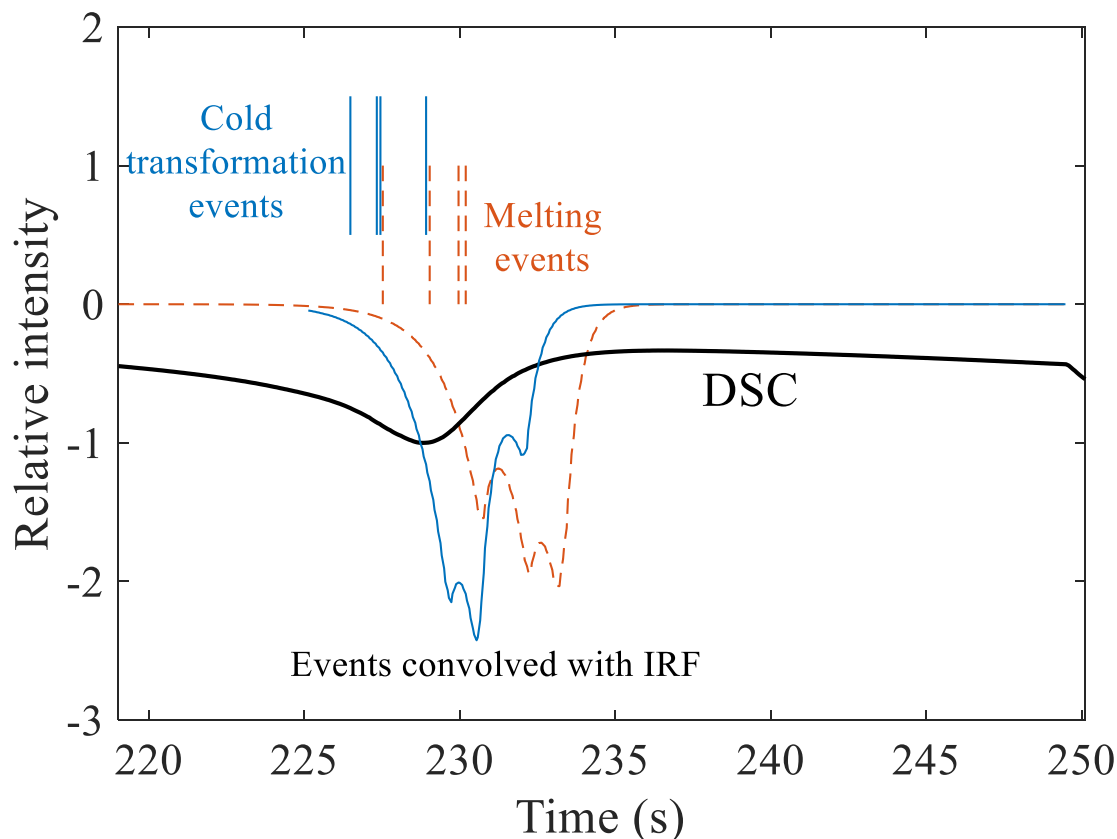


Figure S6. IRF Analysis of Trehalose Dihydrate. The final DSC peak in the trehalose dihydrate experiment was analyzed using the IRF recovered from the urea experiment (see **Fig. 3**). The “cold phase transformation” events and the melting events of the four particles were convolved with the best-fit, double-exponential IRF determined from analysis of SDSC data for urea. The results of the convolution are shown in **Figure S6** as colored curves. Neither the cold phase transformation events nor the melting events produced curves that matched well with the DSC peak. This perhaps indicates that the four particles observed using SHG microscopy are not representative of the full population of particles in the sample. A more complete set of phase transformation events would possibly produce a curve that would better match the DSC peak.